



*J. Serb. Chem. Soc.* 78 (2) 265–279 (2013)  
JSCS–4414

## Ferrate(VI) synthesis at a boron-doped diamond anode

MILAN ČEKEREVAC<sup>1\*#</sup>, LJILJANA NIKOLIĆ BUJANOVIĆ<sup>1</sup>,  
ANJA JOKIĆ<sup>2#</sup> and MILOŠ SIMIČIĆ<sup>1</sup>

<sup>1</sup>IHIS Techno-Experts, Batajnički put 23, 11080 Belgrade, Serbia and <sup>2</sup>University of Priština,  
Faculty of Science, Kosovska Mitrovica, Serbia

(Received 9 March, revised 16 October 2012)

**Abstract:** The electrochemical synthesis of ferrate(VI) by the oxidation of iron compounds from alkaline 10 M KOH electrolytes on a boron-doped diamond electrode was examined by cyclic voltammetry between the potentials of the hydrogen evolution reaction and the oxygen evolution reaction. It was shown that the anodic current peak that appeared in iron-free electrolyte at a less positive potential than the potential of the oxygen evolution probably coincides with oxidation of hydrogen in >CH<sub>2</sub> groups and C-sp<sup>2</sup> graphite impurities with formation of >C=O groups in a C-sp<sup>3</sup> diamond structure. Addition of Fe(III) compounds to the electrolyte provoked the formation of an anodic wave on the cyclic voltammograms in the potential region that correlates with the generation of ferrate(VI). It is concluded that the direct electrochemical synthesis of Fe(VI) at a boron-doped diamond anode is possible because of the less positive potential of ferrate(VI), FeO<sub>4</sub><sup>2-</sup>, formation with respect to the potential of the oxygen evolution reaction. The presence of ferrate(VI) in the electrolyte, formed after anodic polarization of the boron electrode in 10 M KOH electrolyte saturated with Fe(III) at 0.9 V against Hg/HgO electrode, was proven by UV–Vis spectrometry.

**Key words:** ferrate(VI); boron-doped diamond electrode; synthesis; alkaline electrolyte; cyclic voltammetry; UV–Vis spectrophotometry.

### INTRODUCTION

Ferrate(VI) anion, FeO<sub>4</sub><sup>2-</sup>, as a strong environmentally friendly oxidant, has already found numerous applications in environment friendly chemistry, particularly in the processes of polluted water treatment.<sup>1,2</sup> The ferrate(VI) aqueous alkaline solutions obtained by chemical or electrochemical synthesis are the most appropriate reactants for a treatment of a large number of water pollutants. However, ferrates (VI) quite rapidly oxidize water even in strong alkaline water solu-

\* Corresponding author. E-mail: ihis@eunet.rs

# Serbian Chemical Society member.

doi: 10.2298/JSC120309108C

tions and decompose to Fe(III), thereby gradually losing their decontamination capacity. Hence, the direct electrochemical synthesis of ferrate(VI) in the decontaminating reactor by oxidation of Fe(III) compounds at a diamond electrode could solve many technical problems of its practical applications. This could be particularly suitable in cases of the water treatment processes where Fe(II) and Fe(III) salts are used to form Fe(III) hydroxide, an efficient absorbent, coagulant and flocculent, which can be used simultaneously as a reactant for the synthesis of ferrate(VI). The boron-doped diamond (BDD) is one of several suitable dimensionally stable electrode (DSE) materials, which could be utilized for electrochemical synthesis of ferrate(VI) from alkaline solutions of Fe(III) compounds, because of its high chemical and electrochemical stability in aggressive environment over a wide electrode potential range and wide potential difference between the oxygen evolution reaction (OER) and the hydrogen evolution reaction (HER) of more than 3 V and its relatively high electrical conductivity.<sup>3-7</sup>

As a corrosion resistant material, diamond retains its morphology and stability during long-term cycling between the hydrogen and oxygen evolution potentials in very aggressive media, even in acidic fluoride solutions.<sup>7-9</sup>

The BDD surface is also characterized by a low adsorption capacity, so the double-layer capacitance of diamond is up to one order of magnitude lower than that of glassy carbon.<sup>7</sup>

Therefore, conductive diamond is a promising DSE material and in the last decades, it has been used in the development of applications in three broad areas: *i*) electrochemical synthesis of inorganic and organic compounds; *ii*) polluted water treatment, which includes the purification of wastewater and the disinfection of drinking water and *iii*) electro-analysis and sensor technology.<sup>3-21</sup>

The electrochemical generation of ferrate(VI) by the transpassive anodic oxidation of iron in concentrated alkaline solutions has been studied extensively,<sup>1</sup> but the electrochemical generation of ferrate(VI) by oxidation of iron compounds at inert anodes has been much less explored.<sup>12-15</sup> Recently, the electrochemical generation of ferrate(VI) on diamond anodes by the oxidation of ferric and ferrous compounds from the alkaline and acid solutions at high anodic potentials was reported,<sup>12-15,22</sup> but the authors described the ferrate(VI) synthesis mechanism on diamond as a mediated oxidation of Fe(III) to Fe(VI) by electrochemically generated hydroxyl radicals at high anodic potential, because of the chemical inertness of diamond.<sup>12-15</sup>

The possibility of ferrate(VI) generation by a direct anodic oxidation of soluble iron compounds on a diamond electrode from alkaline solutions at lower anodic potentials, which correlates with ferrate(VI) generation by transpassive oxidation of iron, has not hitherto been reported in the relevant literature.

The object of this study was to explore a possibility of ferrate(VI) formation by the direct anodic oxidation of soluble iron(III) compounds on a boron-doped

diamond electrode in alkaline solutions at potentials lower than that of oxygen evolution.

### EXPERIMENTAL

The electrode material, a highly boron-doped diamond layer produced by chemical vapor deposition (CVD) of diamond on a p-silicon wafer plate, was purchased from Element Six Ltd., UK. The synthetic diamond layer was 0.6 mm thick, doped with boron in a concentration  $[B] > 10^{20}$  atoms  $\text{cm}^{-3}$  and with specific resistivity of 0.020–0.18  $\Omega$  cm.

The working electrode was made by fixing of the p-silicon substrate plate on which the BDD layer had been deposited to a copper plate current collector with conductive silver adhesive to secure electrical contact. The inactive back and lateral surfaces of the electrode are insulated from the electrolyte using chemically resistant epoxy resin. The area of the exposed active surface of the electrode was 1  $\text{cm}^2$ .

The BDD electrode surface was washed with ethanol and rinsed with distilled water before each experiment.

The electrode potentials were measured against a red mercuric oxide (Hg|HgO) reference electrode filled with 10 M KOH electrolyte ( $E_0 = 0.095$  V vs. SHE) connected to the working electrode via a Luggin capillary electrolyte bridge.

The auxiliary electrode was a coiled platinum wire.

Cyclic voltammetry experiments were performed using a computer-controlled potentiostat–galvanostat PAR 273 and Gamry G300.

The electrolyte was prepared with p.a. grade chemicals in distilled water. Ferrous sulfate was used for electrolyte preparation because of its higher solubility with respect to those of ferric salts.

The electrolyte compositions labeled on the cyclic voltammetry diagrams denote initial electrolyte composition from which a particular electrolyte is prepared according to the following procedure.

The colloid suspension of  $\text{Fe}(\text{OH})_3$  ( $\text{p}K_s = 38$  at 25 °C for  $[\text{Fe}(\text{OH})_3] = 10$  mM)<sup>23</sup> in concentrated alkaline solution, has been prepared before each experiment by oxidation of 10 M KOH solution saturated with ferrous sulfate by intensive aeration and agitation by means of a laboratory magnetic stirrer. The oxidation of ferrous hydroxide to ferric hydroxide follows change of the solution color from a pale greenish color of Fe(II) to an orange–brown color of Fe(III). Oxidation of the Fe(II) residues in the electrolyte is performed by addition of a stoichiometric quantity of hydrogen peroxide to the previously aerated solution. Finally, the electrolyte was stabilized for at least two hours before electrochemical experiments.

### RESULTS AND DISCUSSION

#### *Crystallography of BDD*

The crystallography of the BDD electrode was examined by X-ray diffraction, Fig. 1, recorded on a Philips PW 1710 X-ray analyzer, prior to and after electrochemical experiments to verify its stability in the experimental environment. The X-ray diffraction patterns illustrate that the main crystallographic parameters of the diamond electrode crystal lattice are generally unchanged after 10 h anodic polarization at  $j = 100$  mA  $\text{cm}^{-2}$  in 10 M KOH solution, which confirmed the structural stability of the BDD material. However, both the decrease in

the intensity of the diffraction peaks and the slight increase in the lattice parameter indicated consumption of the electrode material after prolonged exploitation, but during the short-time CV experiments used, the BDD electrode could be considered as stable.

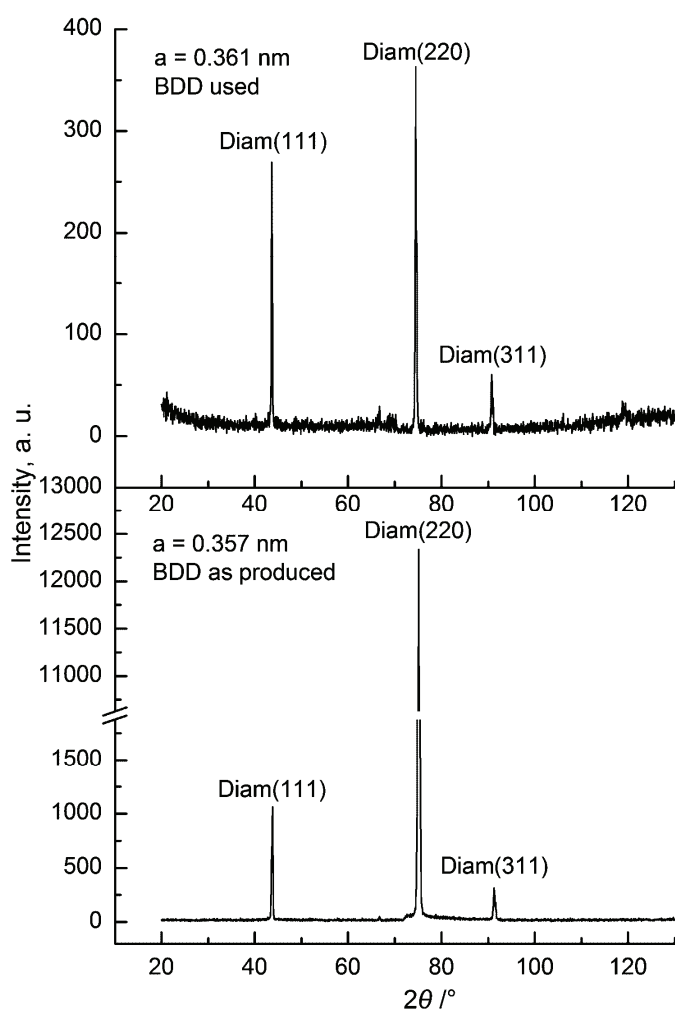


Fig. 1. X-Ray diffraction pattern of the new and the BDD electrode after 10 h anodic polarization at  $j = 100 \text{ mA cm}^{-2}$ ,  $\theta$  – XRD diffraction angle,  $a$  – crystal lattice parameter.

#### *Electrochemical behavior of the BDD electrode in 10 M KOH*

The focus of the preliminary experimental work was the behavior of the BDD electrode in the potential region between the OER and the HER in 10 M KOH electrolyte free of iron ions.

The cyclic voltammograms in Fig. 2 show a steady decline of the anodic current peak, which appeared before the OER potential in the anodic scan direction. This behavior could be the result of the oxidation of inclusions at the diamond surface, C-sp<sup>2</sup> and >CH<sub>2</sub> groups. C-sp<sup>2</sup> groups are usually present in commercial highly boron-doped diamond because of the secondary carbon deposition during the doping process, while the >CH<sub>2</sub> groups are formed on the diamond during cathodic polarization.<sup>7,23–27</sup>

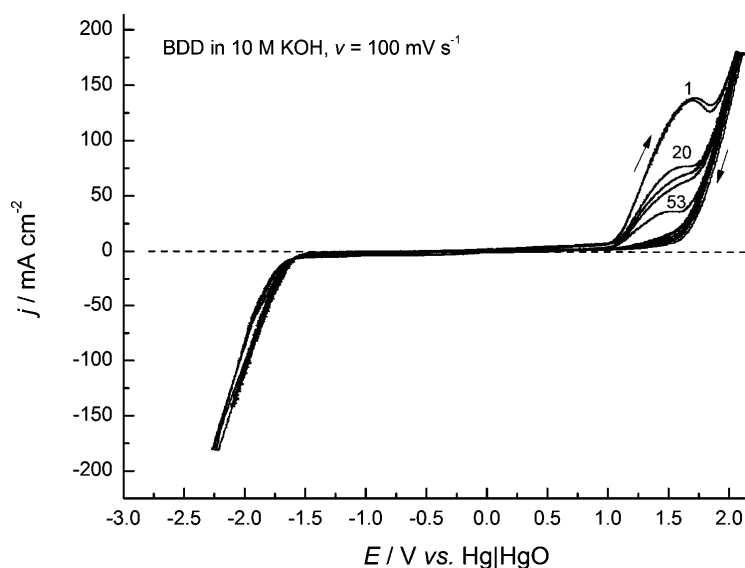
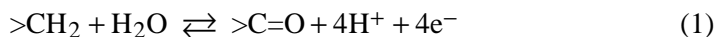


Fig. 2. Cyclic voltammogram of BDD in 10 M KOH,  $\nu = 100 \text{ mV s}^{-1}$ ,  $E_0 = -0.5 \text{ V vs. Hg|HgO}$  after holding potential  $-1.2 \text{ V vs. Hg|HgO}$  for 45 min, scan No. 1 to 53.

The cyclic voltammogram of the BDD electrode obtained after an anodic potential scan limit was set before the potential of the current peak is shown in Fig. 3. The gradual increase of the two peaks, A<sub>1</sub> and A<sub>2</sub>, seen in the enlarged segment of cyclic voltammogram, reflects the incomplete anodic oxidation of the >CH<sub>2</sub> groups according to Eq. (1). The accumulation of >CH<sub>2</sub> groups on the diamond surface is an obvious result of the incomplete oxidation because of the anodic potential scan limit:<sup>15–24</sup>



The results shown in Figs. 2 and 3 are comparable with data reported by Beck *et al.*<sup>26,27</sup>, where the current peak on the cyclic voltammogram of a BDD electrode that appears at the anodic potential scan before the OER potential was explained as being the consequence of the oxidation of both the >CH<sub>2</sub> groups and the graphite impurities from the electrode surface.<sup>26,27</sup>

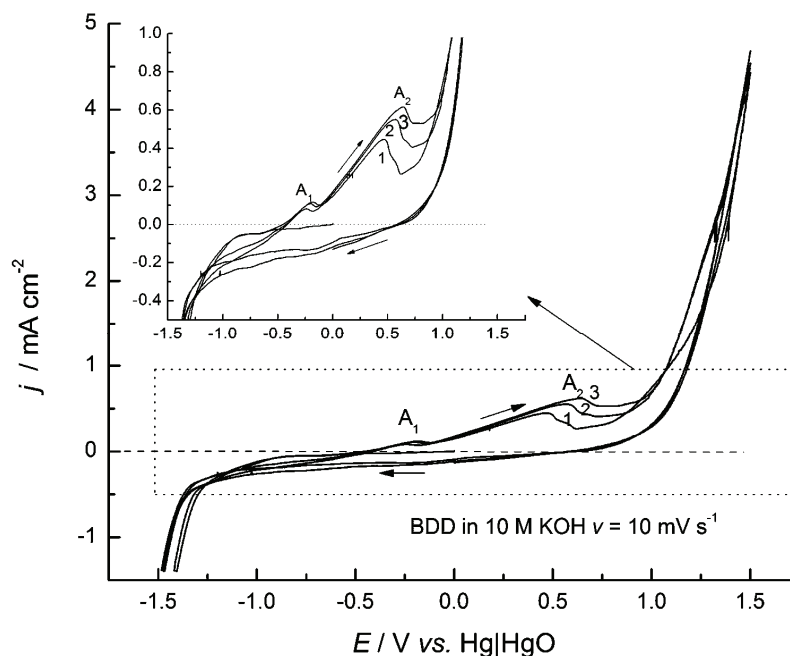


Fig. 3. Cyclic voltammogram for BDD electrode in 10 M KOH solution in the cycle that was limited at an anodic potential before the OER,  $v = 10 \text{ mV s}^{-1}$ .

The third possibility for the appearance of this anodic peak on the voltammogram shown in Fig. 2 would be a lower OER overvoltage on the C-sp<sup>2</sup> surface inclusions. Therefore, polarization of the BDD electrode at higher overpotential than the OER potential is required to oxidize and remove all of these impurities from the electrode surface.<sup>7,26–39</sup>

#### *Electrochemical oxidation of Fe(III) on BDD*

The initial conditions for the electrochemical synthesis of ferrate(VI) by anodic oxidation of ferric species on a BDD electrode in strong alkaline solution were explored by cyclic voltammetry in order to examine the influence of possible parallel processes, such as oxidation of >CH<sub>2</sub> and C-sp<sup>2</sup> and oxygen evolution, on ferrate(VI) production.<sup>1,3–15</sup>

The voltammograms in Fig. 4 show the effect of the presence of ferric compounds in the 10 M KOH alkaline solution on the behavior of the BDD electrode. The behavior of BDD electrode in pure solution is shown on CV (1), and behavior in the presence of Fe(III) species on CV (2). Obviously, Fe(III) species in the alkaline electrolyte provoked the appearance of a current hump or shoulder on the voltammogram (2) at anodic potentials higher than 0.7 V against the Hg|HgO electrode, which is less positive with respect to the potential of the OER in Figs. 2 and 3. Hence, this anodic wave could be the result of the oxidation of

the ferric species to ferrate(VI) precursors, *i.e.*, Fe(IV) or Fe(V), according to Eqs. (2) to (7),<sup>40–49</sup> because in the electrolyte preparation process, all ferrous species were oxidized to ferric species. Thus, there should be no doubt that the growth of the anodic current peak at potentials  $>0.7$  V against the Hg|HgO reference electrode was the result of Fe(III) oxidation to higher valence states, Fe(IV) or Fe(V), which are quoted in the relevant literature as ferrate(VI) precursors.<sup>1,22,40–49</sup>

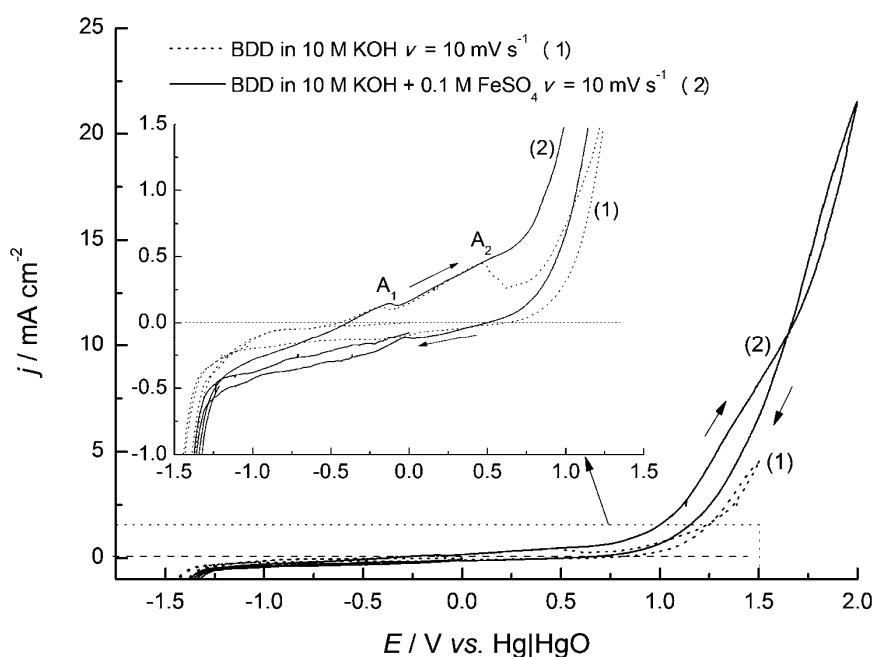


Fig. 4. Cyclic voltammograms of BDD in 10 M KOH (1) and in 10 M KOH + 0.1 M  $\text{FeSO}_4$  (2),  $\nu = 10 \text{ mV s}^{-1}$ .

The cyclic voltammogram of the BDD electrode in 5 M KOH electrolyte saturated with Fe(III) hydroxide, presented in Fig. 5, was obtained with a higher potential scan rate and more clearly demonstrates the possibility of ferrate(VI) synthesis at anodic potentials  $>0.7$  V against the Hg|HgO reference. The current shoulder  $A_2$  is in the potential region that correlates with ferrate(VI) generation, and the corresponding cathodic wave  $C_2$  reflects the reduction of Fe(VI) to Fe(III) and wave  $C_1$  reflects the reduction of Fe(III) to Fe(II).<sup>40–49</sup> The relatively low current density of the Fe(VI) reduction is the result of both ferrate(VI) migration from the electrode, which was observed during the experiment as a characteristic red–purple coloring of the solution in the vicinity of the BDD anode, and the decomposition of adsorbed ferrate(VI) in the reaction with water and Fe(III).<sup>40–49</sup>

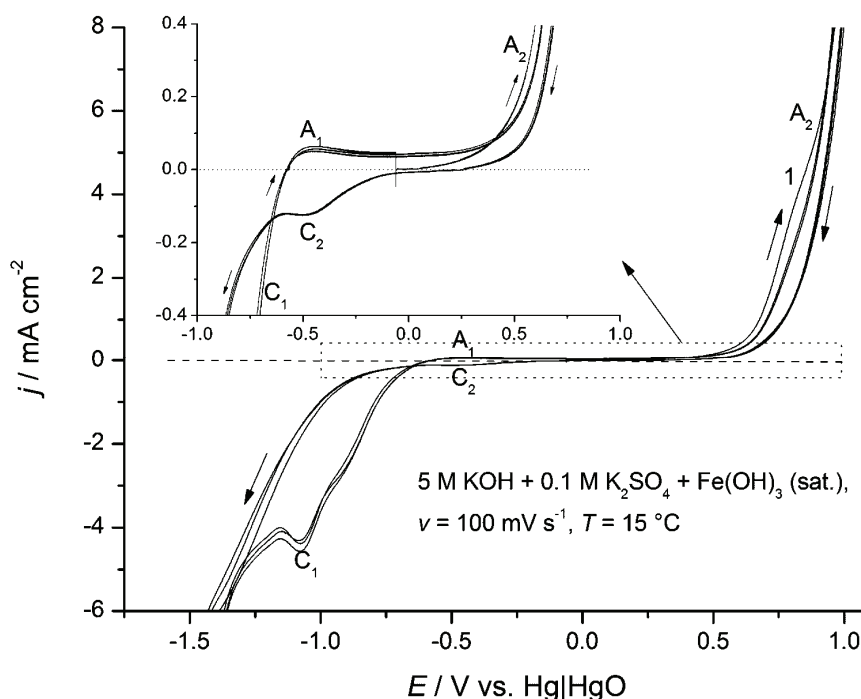


Fig. 5. Cyclic voltammograms of BDD in 5 M KOH + 0.1 M K<sub>2</sub>SO<sub>4</sub> + Fe(OH)<sub>3</sub> (saturated suspension),  $\nu = 100 \text{ mV s}^{-1}$ ,  $T = 15 \text{ }^\circ\text{C}$ .

The cyclic voltammograms in Fig. 6 show the effect of 10 M KOH electrolyte saturated with Fe(OH)<sub>3</sub> on the behavior of the BDD electrode. The potential of the current shoulder on voltammogram (1) shows that Fe(III) compounds are oxidized with formation of ferrate(VI) (observed as a red–purple coloration of the electrolyte) at anodic potentials higher than +0.7 V *vs.* the Hg|HgO electrode, while, according to voltammogram (2), oxidation of >CH<sub>2</sub>, >C=O and the OER on the BDD electrode commence at anodic potentials higher than 1 V. The shift of HER reaction potential more than 0.5 V towards positive potentials on the voltammogram (1) is a consequence of the lower HER overvoltage on deposited iron from iron containing electrolyte, with respect to voltammogram (2) of a clean BDD electrode obtained in an iron-free electrolyte.

The cathodic current peak that appears within the potential region between –200 and –500 mV *vs.* the Hg|HgO reference electrode that is seen on the voltammograms in Figs. 4, 5 and 7, reflects the reduction of ferrate(VI) ions to Fe(III). Namely, the results from the relevant literature show that these current peaks were recorded only if ferrate(VI) had been detected in the electrolyte.<sup>1,22,40–59</sup> The potential region where the ferrate(VI) reduction peak appears depends on numerous variables, such as the electrode material, the electrolyte pH value, the



ferrate(VI) concentration at the electrode surface, the transport of electrode reactants, rate of potential scan, *etc.*<sup>40–49</sup>

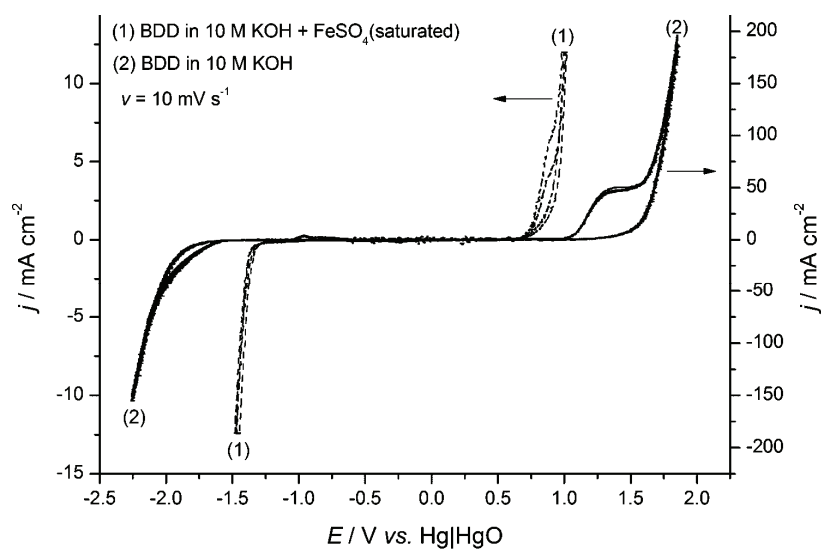


Fig. 6. Cyclic voltammogram of BDD in (1) 10 M KOH saturated with  $FeSO_4$  and (2) 10 M KOH,  $v = 10 mV s^{-1}$ .

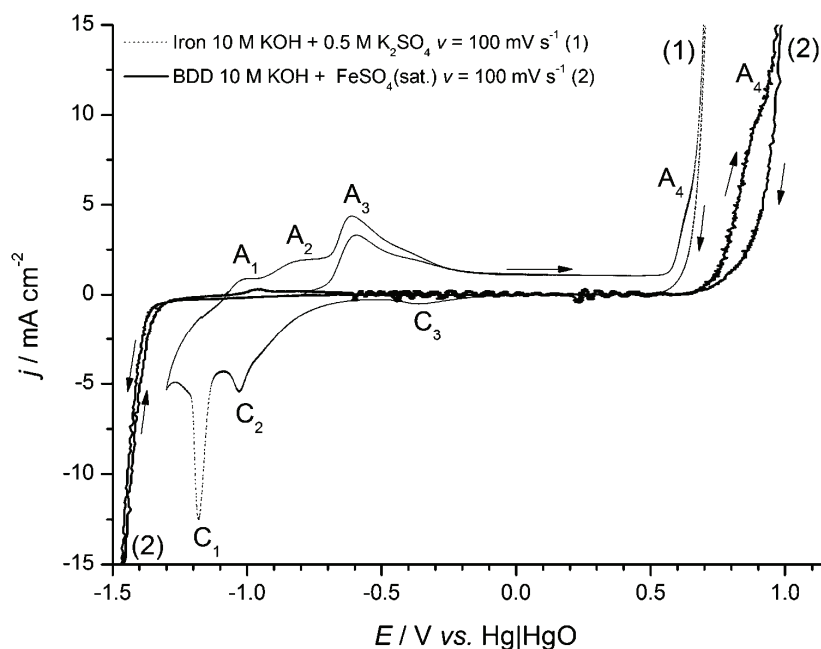


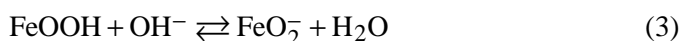
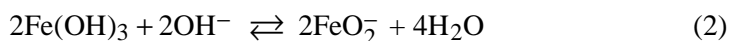
Fig. 7. Cyclic voltammograms of BDD in 10 M KOH +  $FeSO_4$  (saturated) and ARMCO iron (99.99 % Fe) in 10 M KOH, obtained at  $v = 100 mV s^{-1}$ .

The potentials of the current peaks in the region of the ferrate(VI) generation potential shown in Figs. 4–6 are compatible with the results obtained for the anodic oxidation of  $\text{FeO}_2^-$  at an  $\text{SnO}_2\text{--Sb}_2\text{O}_3/\text{Ti}$  electrode,<sup>48</sup> where the authors explained the possibility of ferrate(VI) synthesis at inert electrodes by direct oxidation of ferric compounds.

The cyclic voltammograms in Fig. 7 are given to compare the behavior of an iron electrode in 10 M KOH + 0.5 M  $\text{K}_2\text{SO}_4$  with behavior of the BDD electrode in 10 M KOH electrolyte saturated with soluble ferric species and aid the discussion concerning the mechanism of ferrate(VI) formation at inert anodes. The current waves or shoulders  $A_4$  of ferrate (VI) formation are visible on both voltammograms in Fig. 7. The cathodic current peaks,  $C_3$  of Fe(VI) to Fe(III) reduction,  $C_2$  of Fe(III) to Fe(II) reduction and  $C_1$  that correspond to Fe(II) to Fe(0) reduction are visible only on the iron electrode voltammogram.<sup>40–49</sup> Peak  $A_1$  at the potential of iron oxidation to Fe(II) was noticed on both voltammograms. Peaks  $A_2$  and  $A_3$ , which correlate with the formation of higher valence state iron compounds are seen just on the Fe voltammogram, because ferric compounds are already present in the electrolyte from which ferrate(VI) is formed at a diamond electrode.<sup>40–49</sup>

The overpotential of ferrate(VI) formation by direct anodic oxidation of Fe(III) on a BDD electrode was shifted anodically by approximately 0.2 V with respect to synthesis by transpassive anodic oxidation of iron, as a consequence of a limited availability of soluble Fe(III) reactants at the BDD electrode.<sup>12–15,22,40–49</sup> That is, the rate of ferrate(VI) generation at inert anodes is limited by a low concentration of soluble Fe(III) compounds and hence its low migration rate towards the electrode.

Due to the low solubility product constant of  $\text{Fe}(\text{OH})_3$ ,  $2.79 \times 10^{-39}$  in pH 8 solutions, the electrochemical generation of Fe(VI) by oxidation of Fe(III) at a BDD seems improbable, but in solutions with high a concentration of  $\text{OH}^-$ ,  $\text{Fe}(\text{OH})_3$  and  $\text{FeOOH}$  behave like weak acids and succumb to acidic ionization according to Eqs. (2) and (3) with the formation of  $\text{FeO}_2^-$ , the most soluble form of Fe(III).<sup>12–15,40–50</sup> The concentration of  $\text{FeO}_2^-$  can reach the considerably large values of 0.02 M in 14 M NaOH in the presence of oxidants,<sup>48</sup> which would also be the case in this study because of an oxidative environment:

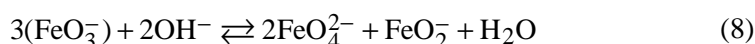
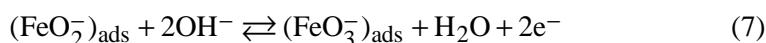
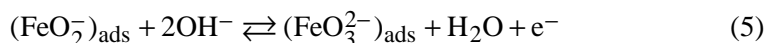


As BDD is a rather inert anode material with low adsorption capacity,<sup>3–15</sup> the adsorption rate of reacting Fe(III) species on the BDD surface, Eq. (4), also controls the rate of ferrate(VI) synthesis:



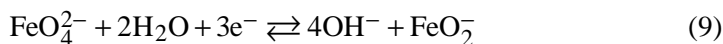
According to the relevant literature,  $\text{FeO}_2^-$  will be oxidized in strong alkaline solutions to  $\text{Fe}^{\text{IV}}\text{O}_3^{2-}$  according to Eq. (5) or  $\text{Fe}^{\text{V}}\text{O}_3^-$  according to Eq. (7), depending on the experimental conditions.<sup>12-15,45-50</sup>

The precursors  $\text{Fe}^{\text{IV}}\text{O}_3^{2-}$  and  $\text{Fe}^{\text{V}}\text{O}_3^-$  finally disproportionate to ferrate(VI) –  $\text{Fe}^{\text{VI}}\text{O}_4^{2-}$  and ferrate(III) –  $\text{Fe}^{\text{III}}\text{O}_2^-$ , in the processes given by Eqs. (6) and (8), respectively.

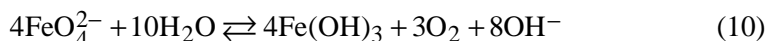


Adsorption of sulfates, which are formed in the hydrolysis process of ferrous salts, at a BDD electrode may have some weak effect on the adsorbed Fe(III) oxide structure,<sup>50</sup> but as the oxidation of sulfate starts at higher positive potentials than the potential of ferrate(VI) generation, this would not influence its generation.<sup>7,3-21</sup>

At cathodic polarization, ferrate(VI) is reduced to Fe(III) according to reaction given by Eq. (9):



Although ferrate(VI) is relatively stable in strong alkaline solutions, cathodic ferrate(VI) small reduction current peaks on the cyclic voltammograms of BDD Figs. 4, 5 and 7 were visible. This could be a consequence of ferrate(VI) migration from the inert anode and the catalytic effect of  $\text{FeO}_2^-$  present in the electrolyte on its decomposition, according to the reversible reactions given by Eqs. (6) and (8), and of water oxidation, according to Eq. (10), which together cause a considerable decrease in the surface concentration of ferrate(VI):<sup>1,12-14,22,40-49</sup>



The formation of the ferrate(VI) by anodic oxidation of ferric compounds at the BDD electrode in strong alkaline solution was confirmed by the UV-Vis absorbance spectra of the ferrate(VI) solutions. The UV-Vis absorbance spectrum of a 0.03 mM  $\text{FeO}_4^{2-}$  solution in 10 M KOH is presented in Fig. 8, on which the characteristic absorbance peak of  $\text{FeO}_4^{2-}$  at 504 nm is obvious.<sup>51</sup> The 0.03 mM  $\text{FeO}_4^{2-}$  ferrate(VI) solution was prepared by the anodic polarization of the BDD electrode for 2 h at a potential of 0.9 V vs. the Hg|HgO reference electrode in 10 M KOH electrolyte saturated with  $\text{Fe}(\text{OH})_3$  with an average current intensity of 10 mA. A current efficiency of 25 % was determined by the chromite analytical method.<sup>52-53</sup>

The experimental results and the discussion on a possible mechanism of ferrate(VI) electrochemical synthesis at inert anodes given in this study disagree with the results and discussion of Sánchez-Carretero *et al.*,<sup>14,15</sup> who explained the formation of ferrate(VI) at a BDD electrode as the result of a mediated Fe(III) oxidation by hydroxyl radicals at high anodic potentials. The results of this study show that an anodic synthesis of ferrate(VI) at a BDD is possible at a lower anodic potential with respect to the potential of the OER. In addition, the formation of hydroxyl radicals is only possible at anodic potential higher than the potential of the OER,<sup>7,36–39</sup> and, especially, higher than the overpotential of Fe(III) oxidation and ferrate(VI) formation.<sup>40–49</sup> Moreover the electro-chemical generation of hydroxyl radicals at BDD electrode pH >9 electrolytes was not evidenced.<sup>39</sup>

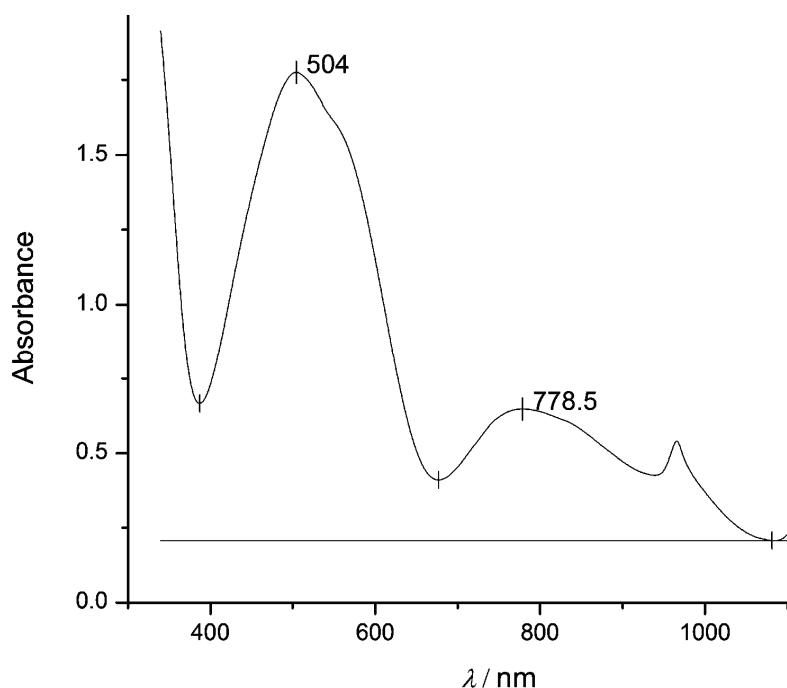


Fig. 8. UV-Vis Absorbance spectra of the ferrate(VI) solution obtained by anodic oxidation of saturated Fe(III) alkaline solution 10 M KOH on BDD electrode at 0.9 V vs. Hg|HgO for 2 h and  $I \approx 10$  mA.  $\lambda$  is the wavelength.

#### CONCLUSIONS

The possibility of the direct electrochemical synthesis of ferrate(VI) by oxidation of Fe(III) species in a 10 M KOH solution on a BDD anode was explored by cyclic voltammetry.

The influences of factors such as the surface coverage of the BDD electrode with  $>\text{CH}_2$  and  $>\text{C}=\text{O}$ , the overpotential of oxygen evolution, as well as the rates

of formation, transport and adsorption on the BDD of soluble Fe(III) compounds, such as  $\text{FeO}_2^-$ , on the anodic synthesis of ferrate(VI) have been discussed.

Ferrate(VI) formation by direct oxidation of soluble Fe(III) compounds on a BDD electrode is possible at a lower anodic potential with respect to the oxygen evolution reaction potential.

Formation of ferrate(VI) by anodic oxidation of Fe(III) from strong alkaline solution at a BDD electrode was confirmed by the characteristic peak of ferrate(VI) in the UV-Vis absorbance spectra of the synthesized ferrate(VI) solution.

*Acknowledgements.* Authors appreciate that this work was partly financed by the Ministry of Education, Science and Technological Development of the Republic of Serbia through projects TR 34025 "Development of ecological processes, based on the application of ferrate(VI) and electrochemical oxidation and reduction, for treatment of harmful substances" and TR 31080 "Biodiversity as a potential in eco-remediation technologies of harmed ecosystems". The Authors also wish to thank the anonymous reviewers for their valuable suggestions.

#### ИЗВОД

#### СИНТЕЗА ФЕРАТА(VI) НА БОРИРАНОЈ ДИЈАМАНТСКОЈ ЕЛЕКТРОДИ ИЗ НЕУТРАЛНИХ И АЛАКАЛНИХ ЕЛЕКТРОЛИТА

МИЛАН ЧЕКЕРЕВАЦ<sup>1</sup>, ЉИЉАНА НИКОЛИЋ-БУЈАНОВИЋ<sup>1</sup>, АЊА ЈОКИЋ<sup>2</sup> и МИЛОШ СИМИЧИЋ<sup>1</sup>

<sup>1</sup>*INIS Techno-experts, Бајајнички пут 23, 11080 Београд и* <sup>2</sup>*Универзитет у Приштини, Природно-математички факултет, Косовска Митровица*

Испитивана је оксидација једињења гвожђа на борираној дијамантској електроди у алкалном електролиту 10 М КОН методом цикличне волтаметрије, између потенцијала реакције издвајања водоника и потенцијала реакције издвајања кисеоника, са циљем електрохемијске синтезе ферата (VI). Показано је да врхови анодних струја који се јављају у електролиту без гвожђа при мање позитивним потенцијалима од потенцијала реакције издвајања кисеоника, вероватно одговарају оксидацији  $>\text{CH}_2$  група и  $\text{C-sp}^2$  графитних нечистоћа уз настајање  $>\text{C}=\text{O}$  група у  $\text{C-sp}^3$  дијамантској структури. Додатак Fe(III) једињења у електролит изазива формирање анодног таласа на цикличним волтамограмима у области потенцијала који одговара настајању ферата(VI). Закључено је да је директна електрохемијска синтеза Fe(VI) једињења на борираној дијамантској аноди могућа услед мање позитивног потенцијала формирања ферата(VI) у односу на потенцијал реакције издвајања кисеоника. Присуство ферата(VI) формираног након анодне поларизације бориране дијамантске електроде у електролиту 10 М КОН засићеном једињењима Fe (III) на 0,9 V у односу на Hg|HgO електроду доказано је UV-Vis спектрометријом.

(Примљено 9. марта, ревидирано 16. октобра 2012)

#### REFERENCES

1. V. K. Sharma. Ed., *Ferrates*, ACS Symposium Series 985, American Chemical Society, Washington, DC, USA, 2008
2. M. I. Čekerevac, L. N. Nikolić-Bujanović, M. B. Mirković, N. H. Popović, *Hem. Ind.* **64** (2010) 423

3. G. M. Swain, A. B. Anderson, J. C. Angus, *MRS Bull.* **23** (1998) 56
4. H. B. Martin, A. Argoitia, U. Landau, A. B. Anderson, J. C. Angus, *J. Electrochem. Soc.* **143** (1996) 133
5. M. Panizza, G. Cerisola, *Electrochim. Acta* **51** (2005) 191
6. A. Kraft, *Int. J. Electrochem. Sci.* **2** (2007) 355
7. B. Marselli, *Electrochemical oxygen transfer reaction on Synthetic boron-doped diamond thin film electrode*, Thèse No. 3057, École Polytechnique Fédérale de Lausanne, Lausanne, 2004
8. G. M. Swain, *J. Electrochem. Soc.* **141** (1994) 3382
9. R. Ramesham, M. F. Rose, *Diamond Relat. Mater.* **6** (1997) 17
10. G. M. Swain, *Adv. Mater.* **5** (1994) 388
11. G. M. Swain, R. Ramesham, *Anal. Chem.* **65** (1993) 345
12. P. Cañizares, M. Arcís, C. Sáez, M. A. Rodrigo, *Electrochem. Commun.* **9** (2007) 2286
13. C. Sáez, M. A. Rodrigo, P. Cañizares, *AIChE J.* **54** (2008) 1600
14. A. Sánchez-Carretero, M. A. Rodrigo, P. Cañizares, C. Sáez, *Electrochem. Commun.* **12** (2010) 644
15. A. Sánchez-Carretero, C. Sáez, P. Cañizares, S. Cotillas, M. A. Rodrigo, *Ind. Eng. Chem. Res.* **50** (2011) 7073
16. K. Arihara, C. Terashima, A. Fujishima, *Electrochem. Solid-State Lett.* **9** (2006) D17
17. A. Kraft, M. Stadelmann, M. Wünsche, M. Blaschke, *Electrochem. Comm.* **8** (2006) 883
18. P. A. Michaud, E. Mahe, W. Haenni, A. Perret, C. Comninellis, *Electrochem. Solid-State Lett.* **3** (2000) 77
19. T. Lehmann, P. Stenner, Degussa A.G., Düsseldorf (DE), US Patent 6503386 (2003)
20. C. Comninellis, P. A. Michaud, W. Haenni, A. Perret, M. Fryda, US Patent 6855242 (2005)
21. M. Panizza, I. Duo, P. A. Michaud, G. Cerisola, C. Comninellis, *Electrochem. Solid-State Lett.* **3** (2000) 550
22. J. Lee, D. A. Tryk, A. Fujishima, S.-M. Park, *Chem. Commun.* (2002) 486
23. J. Duan, J. Gregory, *Adv. Colloid Interface Sci.* **100–102** (2003) 475
24. M. S. Saha, T. Furuta, Y. Nishiki, *Electrochem. Solid-State Lett.* **6** (2003) D5
25. P. Cañizares, F. Larrondo, J. Lobat, M. A. Rodrigo, C. Sáez, *J. Electrochem. Soc.* **152** (2005) D191.
26. F. Beck, H. Krohn, W. Kaiser, M. Fryda, C. P. Klages, L. Schäfer, *Electrochim. Acta* **44** (1998) 525
27. F. Beck, W. Kaiser, H. Krohn, *Electrochim. Acta* **45** (2000) 4691
28. I. Yagi, H. Notsu, T. Kondo, D. A. Tryk, A. J. Fujishima, *J. Electroanal. Chem.* **473** (1999) 173
29. K. Hayashi, S. Yamanaka, H. Watanabe, T. Sekiguchi, H. Okushi, K. Kajimura, *J. Appl. Phys.* **81** (1997) 744
30. M. C. Granger, G. M. Swain, *J. Electrochem. Soc.* **146** (1999) 4551
31. M. C. Granger, M. D. Koppang, M. Witek, J. E. Butler, J. Xu, G. Lucazeau, J. Wang, M. Hupert, M. Mermoux, A. Hanks, J. W. Strojek, G. M. Swain, *Anal. Chem.* **72** (2000) 3793
32. N. Simon, H. Girard, D. Ballutaud, S. Ghodbane, A. Deneuve, M. Herlem, A. Etcheberry, *Diamond Relat. Mater.* **14** (2005) 1179
33. J. Ristein, *Appl. Phys., A* **82** (2006) 377
34. J. H. T. Luong, K. B. Male, J. D. Glennon, *Analyst* **134** (2009) 1965

35. V. Chakrapani, S. C. Eaton, A. B. Anderson, M. Tabib-Azar, J. C. Angus, *Electrochem. Solid-State Lett.* **8** (2005) E4
36. K. J. McKenzie, F. Marken, *Electrochem. Solid-State Lett.* **5** (2002) E47
37. I. Duo, A. Fujishima, C. Comninellis, *Electrochem. Commun.* **5** (2003) 695
38. K. Serrano, P. A. Machaud, C. Comninellis, A. Savall, *Electrochim. Acta* **48** (2002) 431
39. T. A. Enache, A. M. Chiorcea-Paquim, O. Fatibello-Filho, A. M. Oliveira-Brett, *Electrochem. Commun.* **11** (2009) 1342
40. S. Venkatadri, W. F. Wagner, H. H. Bauer, *Anal. Chem.* **43** (1971) 1115
41. F. Beck, R. Kaus, M. Oberst, *Electrochim. Acta* **30** (1985) 173
42. K. Bouzek, I. Roušar, *J. Appl. Electrochem.* **23** (1993) 1317
43. K. Bouzek, I. Roušar, H. Bergmann, K. Hertwig, *J. Electroanal. Chem.* **425** (1997) 125
44. M. De Koninck, D. Belanger, *Electrochim. Acta* **48** (2003) 1435
45. M. I. Čekerevac, L. N. Nikolić-Bijanović, M. V. Simičić, *Hem. Ind.* **63** (2009) 387
46. Z. Mácova, K. Bouzek, V. K. Sharma, *J. Appl. Electrochem.* **40** (2010) 1019
47. Z. A. Mácová, K. Bouzek, *J. Appl. Electrochem.* **41** (2011) 1125
48. C.-Z. Zhang, Z. Liu, F. Wu, L.-J. Lin, F. Qi, *Electrochem. Commun.* **6** (2004) 1104
49. H. B. Shao, J. M. Wang, W. C. He, J. Q. Zhang, C. N. Cao, *Electrochem. Commun.* **7** (2005) 1429
50. R. M. Cornell, U. Schwertmann, *The Iron Oxides: Structure Properties Reactions Occurrences and Uses*, Wiley-VCH, Weinheim, Germany, 2003, p.p. 3, 221–252
51. S. Licht, V. Naschitz, L. Halperin, N. Halperin, L. Lin, J. Chen, S. Ghosh, B. Liu, *J. Power Sources* **101** (2001) 167
52. J. M. Schreyer, L. T. Ockerman, *Anal. Chem.* **23** (1951) 1312
53. W. F. Wagner, J. R. Gump, E. N. Hart, *Anal. Chem.* **24** (1952) 1497.